

Supporting Information

Low Full-Cell Voltage Driven High-Current-Density Selective Paired Formate Electrosynthesis

Chuqian Xiao ^a, Ling Cheng ^b, Yating Wang ^a, Jinze Liu ^b, Rongzhen Chen ^a, Hao Jiang ^{a*}, Yuhang Li ^{a*}, Chunzhong Li ^{a,b*}

^a Key Laboratory for Ultrafine Materials of Ministry of Education, Shanghai Engineering Research Center of Hierarchical Nanomaterials, Frontiers Science Center for Materiobiology and Dynamic Chemistry, School of Materials Science and Engineering, East China University of Science & Technology Shanghai 200237, China

^b School of Chemical Engineering, East China University of Science & Technology Shanghai 200237, China

* Corresponding authors. E-mails: yuhangli@ecust.edu.cn (Yuhang Li), jianghao@ecust.edu.cn (Hao Jiang), czli@ecust.edu.cn (Chunzhong Li)

Methods

Calculation of energy efficiency

The Gibbs free energy can be converted to standard equilibrium potential (vs. SHE) by Eqn S1:

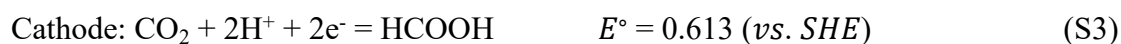
$$\Delta G^\circ = -nFE \quad (\text{S1})$$

Where ΔG° (kJ mol⁻¹) is the Gibbs free energy; n is the number of electrons transferred; F is the Faraday constant (96,485 C mol⁻¹); E° is the standard redox potential of the corresponding redox couples versus the standard hydrogen electrode (SHE).

Nernst equation was used for the calculation of thermodynamic potential by Eqn. S2:

$$E = E^\circ - 0.059 \times pH \quad (\text{S2})$$

The two half-reactions, the overall paired reaction, and the thermodynamic potentials are shown in Eqs. S3–5:



Energy efficiency (ϵ) as a function of cell voltage (V_{cell}) can be calculated by Eqn. S6:

(S6)

$$\epsilon = |E_{\text{cell}}| / V = |FE_{\text{MOR}} * E_{\text{MOR}} - FE_{\text{CO}_2\text{R}} * E_{\text{CO}_2\text{R}}| / V \quad (\text{S6})$$

Calculation of ϵ in the flow cell as an example: 100 mA cm⁻²

In pH 14 KOH solution:

$$\text{MOR: } E = 0.103 - 0.059 \times 14 = -0.723 \text{ V}$$

$$\text{CO}_2\text{RR: } E = 0.613 - 0.059 \times 14 = -0.213 \text{ V}$$

$$\epsilon = |E_{\text{cell}}| FE / V = |FE_{\text{MOR}} * E_{\text{MOR}} - FE_{\text{CO}_2\text{R}} * E_{\text{CO}_2\text{R}}| / V = |1.0046 * (-0.723) - 1.0363$$

$$* (-0.213)| / 2.06 * 100 \% = 24.54 \%$$

Table S1. Comparison of the anodic MOR performance.

Electrocatalysts	Onset potential (V vs. RHE)	Current density at reported potential (mA cm ⁻²)	Reference
S-NiCo-LDH	1.22	100 @ 1.32 V 200 @ 1.36 V 300 @ 1.39 V	This work
Ni-NF	1.30	100 @ 1.35 V	Ref. 1: <i>Adv. Mater.</i> 2021, 33, 2008631
Co(OH) ₂ @HOS/CP	1.30	100 @ 1.53 V	Ref. 2: <i>Adv. Funct. Mater.</i> 2020, 30, 1909610
Ni ₃ S ₂ -CNFs/CC	1.33	100 @ 1.40 V 200 @ 1.44 V	Ref. 3: <i>Nano Energy</i> 2021, 80, 105530
h-NiSe/CNTs	1.35	100 @ 1.45 V 200 @ 1.52 V	Ref. 4: <i>Adv. Funct. Mater.</i> 2021, 31, 2008812
Branched Ni ₃ C	1.43	127 @ 1.67 V	Ref. 5: <i>Angew. Chem. Int. Ed.</i> 2020, 59, 20826
Ni-Mo-N/CFC	/	100 @ 1.52 V	Ref. 6: <i>Nat. Commun.</i> 2019, 10, 5335

* The data are estimated based on the LSV curves given in literature.

Table S2. Comparison of reported full-cell electrolyzers pairing MOR with CO₂RR.

Catalysts	Anodic j_{formate}^* (mA cm ⁻²)	Cathodic j_{formate}^* (mA cm ⁻²)	Full-cell voltage (V)	Energy efficiency (%)	Reference
Anode: S-NiCo-LDH	100	104	2.06	24.54	This work
Cathode: BiPO₄ derived 2D nanosheets	220	175	2.28	26.74	
	300	205	2.48	23.39	
Anode: Ni(OH) ₂ /NF Cathode: Bi	60 100	NA	2.5 3.0	NA	Ref. 7: <i>Chemical Engineering Journal</i> 2021, 412, 127893
Anode: CuONS/CF Cathode: mSnO ₂ /CC	18.3	16.1	1.22	40.00	Ref. 8: <i>Angew. Chem. Int. Ed.</i> 2021, 60, 3148-3155
Anode: Ni(OH) ₂ - NF Cathode: Bi- ene(BDC)	7 14.4 27.5	7.5 15 27	2 2.4 3	25.50 21.25 17.00	Ref. 1: <i>Adv. Mater.</i> 2021, 33, 2008631

* Formate partial current density is calculated by multiplying current density by formate FE.

Supplementary Figures

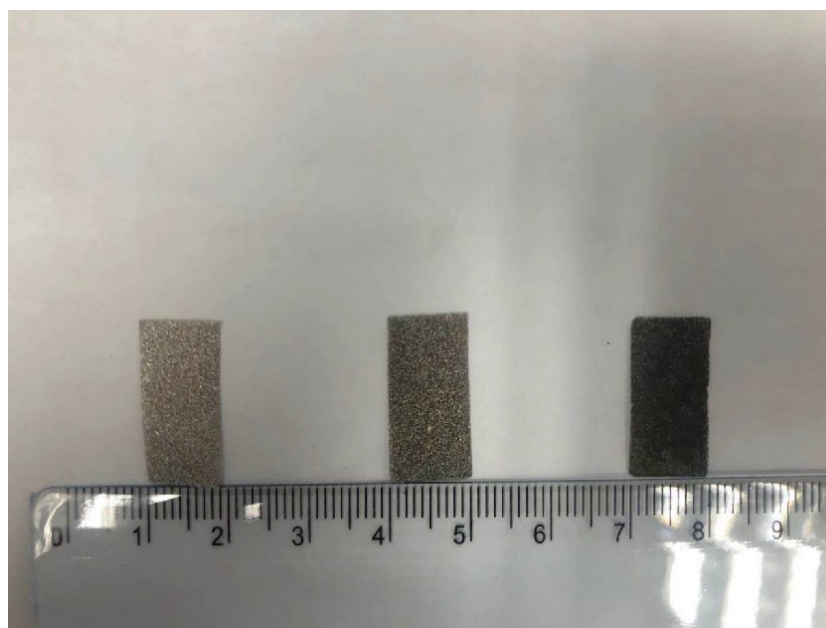


Fig. S1 Digital photos of the bare Ni foam, NiCo-LDH and S-NiCo-LDH (from left to right).

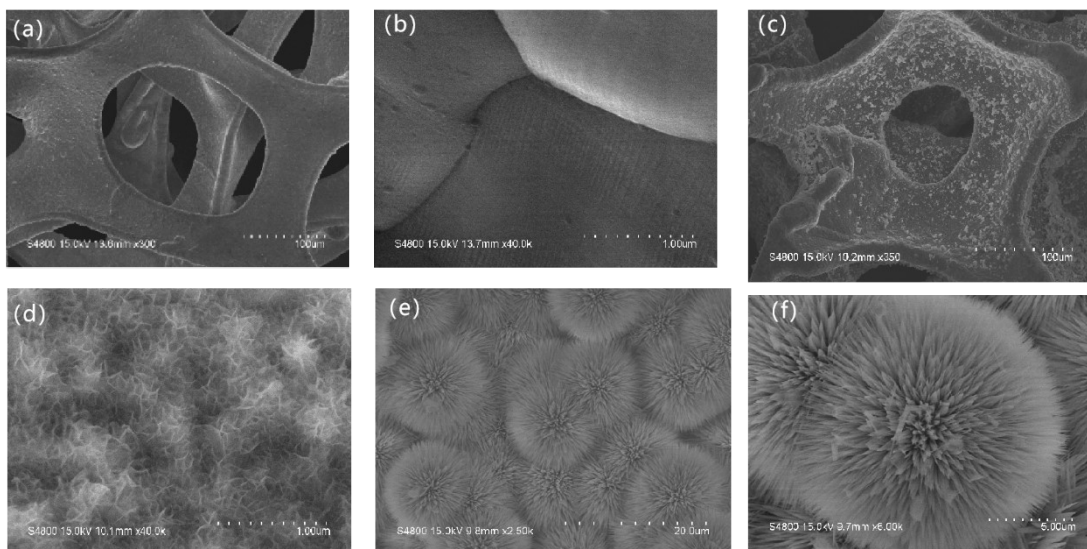


Fig. S2 Low-and high-magnification SEM images of **(a-b)** bare NF, **(c-d)** NiCo-LDH and **(e-f)** NiCo(OH)-HT. The NiCo(OH)-HT sample was prepared by hydrothermal treatment (Methods).

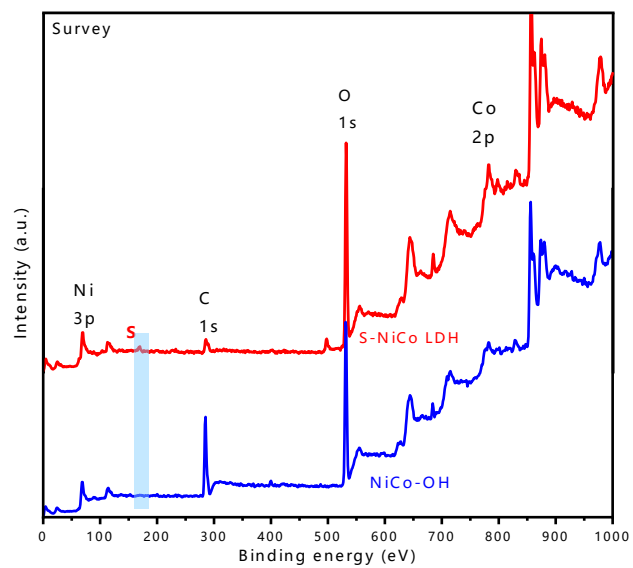


Fig. S3 XPS survey scans of S-NiCo-LDH (red line) and NiCo-LDH (blue line).

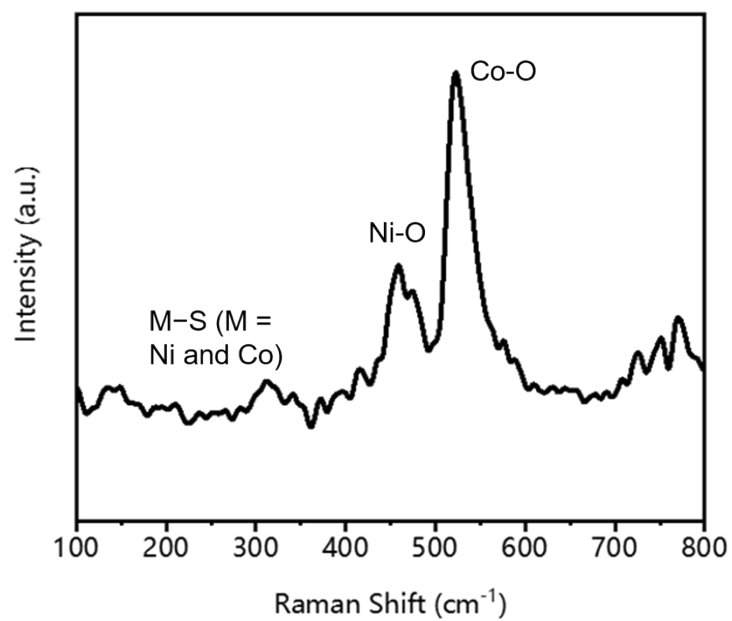


Fig. S4 The Raman spectrum of the S-NiCo-LDH.

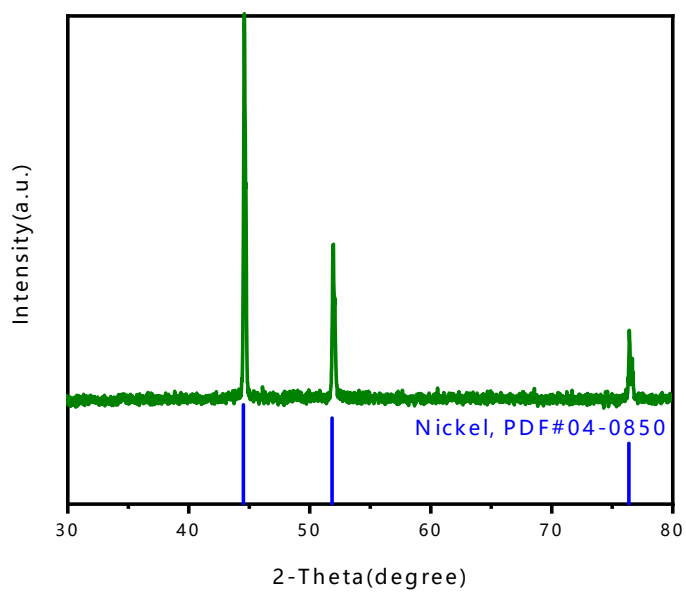


Fig. S5 The XRD pattern of S-NiCo-LDH.

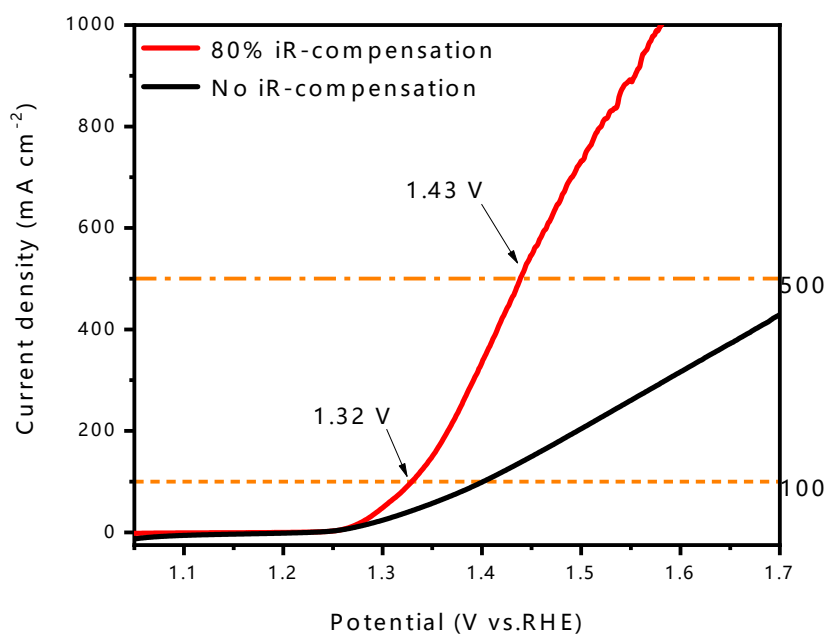


Fig. S6 LSV curves of S-NiCo-LDH with 80% iR-compensation (red line) and without iR-compensation (black line).

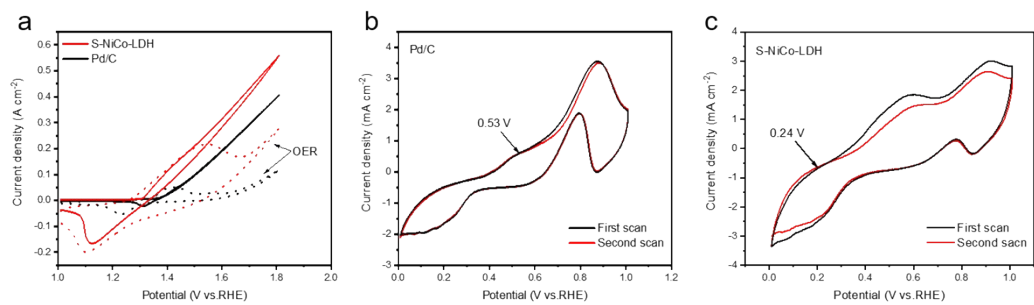


Fig. S7 (a) CV curves in 1.0 M KOH solution with and without 1.0 M methanol. Scan rate: 50 mV s⁻¹. (b) CO stripping tests of commercial Pd/C and (c) S-NiCo-LDH.

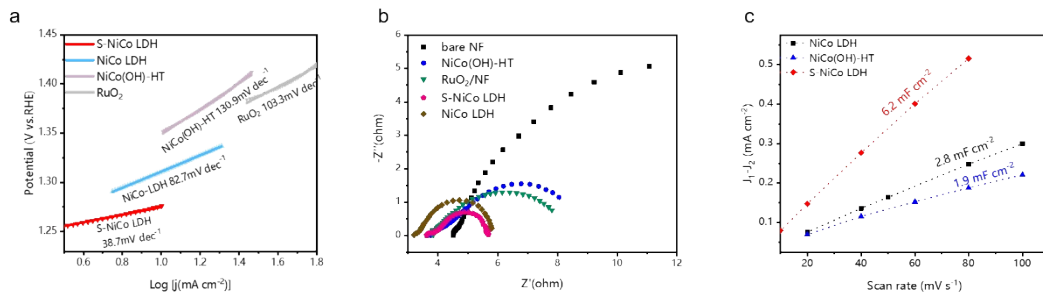


Fig. S8 (a) Tafel plots for the anodic partial MOR derived from the LSV results; **(b)** Nyquist plots obtained from electrochemical impedance spectroscopy (EIS) measurements at a potential of 1.40 V in 1 M KOH mixed with 1 M methanol solution; **(c)** Charging current density differences plotted against scan rates. The linear slope, equivalent to twice the double-layer capacitance C_{dl} , is employed to represent the electrochemically active surface area (ECSA).

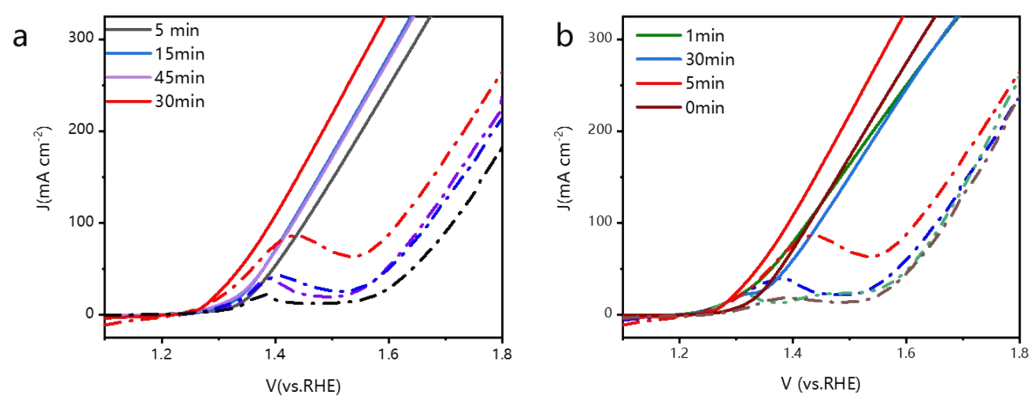


Fig.S9 LSV curves of the S-NiCo-LDH samples prepared by different **(a)** ultraistic and **(b)** sulfurization time.

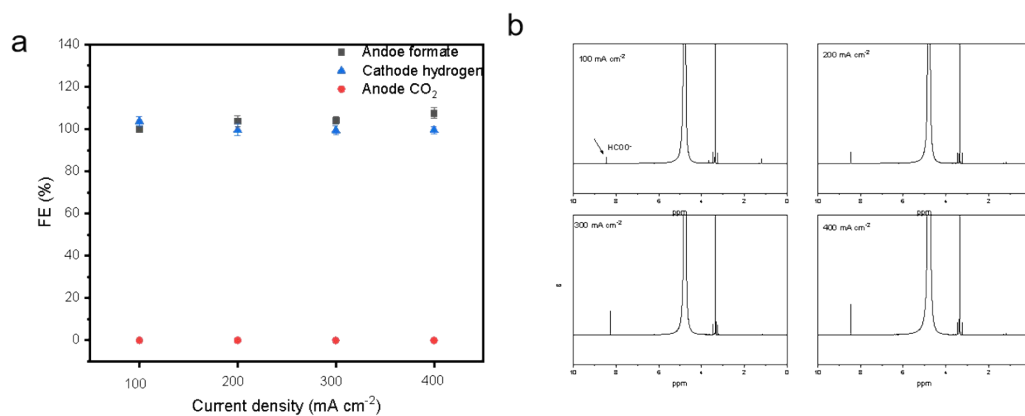


Fig. S10 (a) The calculated FEs of hydrogen, formate and CO₂ for different current density at cathode and anode, respectively. **(b)** ¹H NMR spectra of formate measured from 100-400 mA cm⁻².

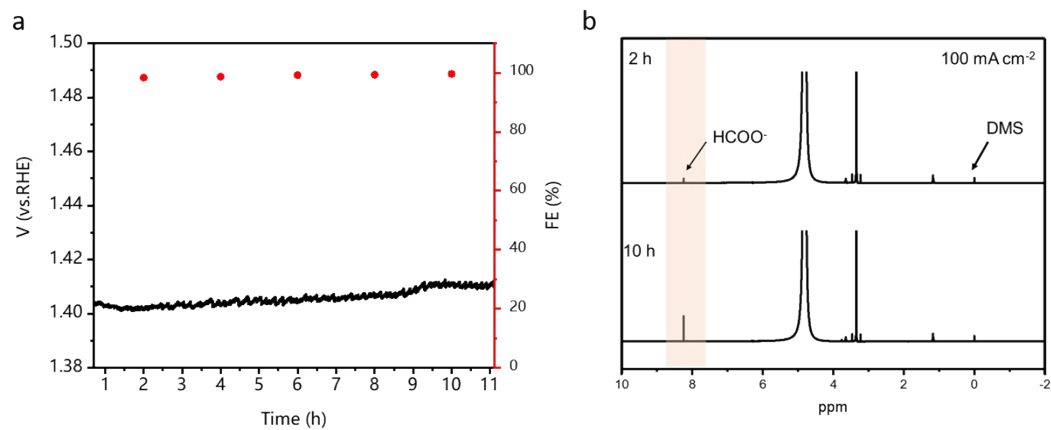


Fig. S11 (a) Stability test of MOR during 11 hours of electrolysis under the current density of 100 mA cm^{-2} . Red dot for formate FE and black line for potential curve. (b) The ^1H NMR spectra of the anode product obtained through the MOR by CP at 100 mA cm^{-2} for 2 hours and 10 hours.

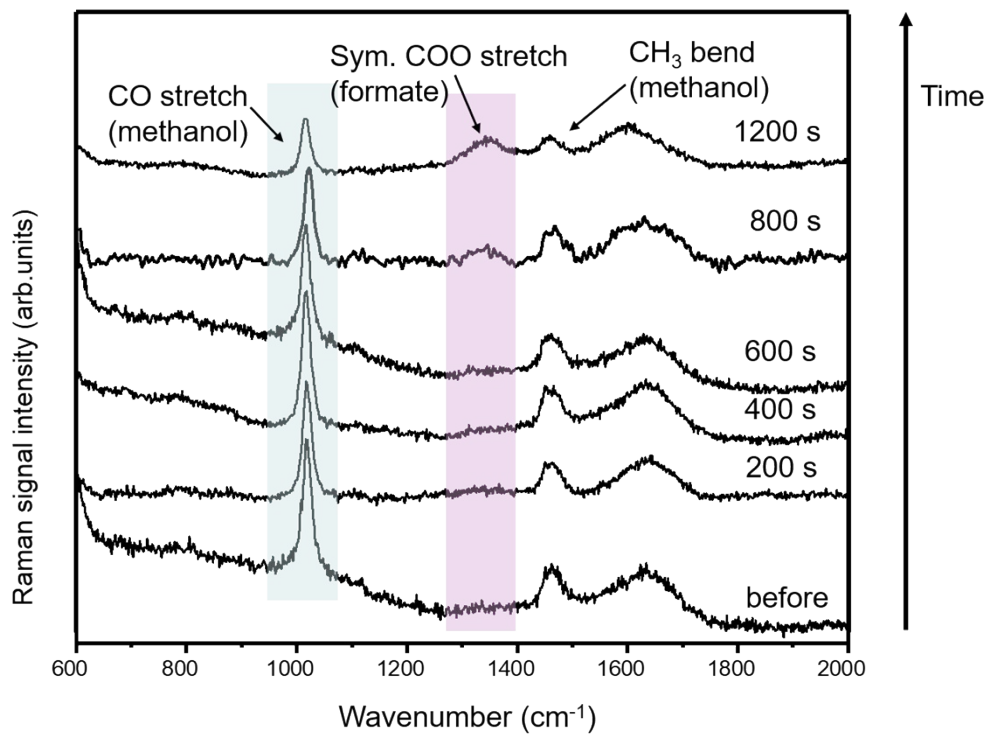


Fig. S12 *Operando* Raman spectra collected under chronopotentiometry (CP) at 25 mA in 1.0 M KOH solution with 1.0 M methanol.

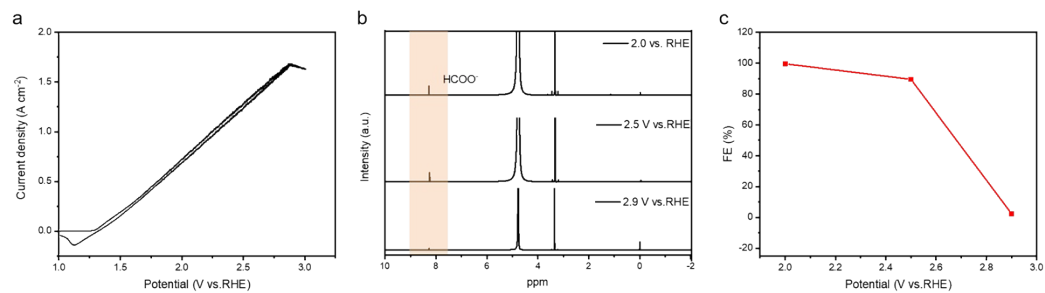


Fig. S13 (a) CV curves in 1.0 M KOH solution with 1.0 M methanol. Scan rate: 50 mV s⁻¹. (b) The ¹H NMR spectrum after CA test. (c) The corresponding faradaic efficiencies for formate at different potentials.

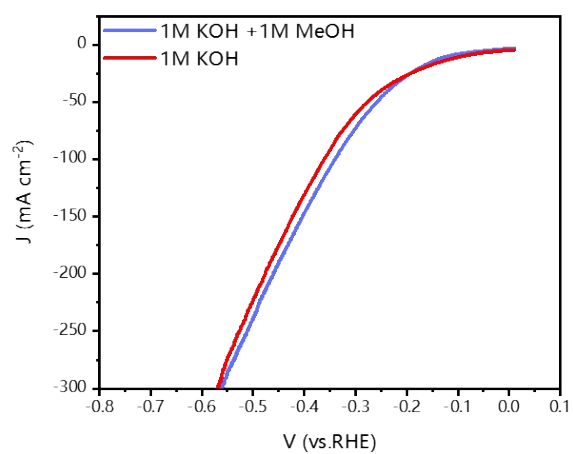


Fig. S14 LSV curves for the HER of S-NiCo-LDH in 1 M KOH with and without 1 M methanol addition.

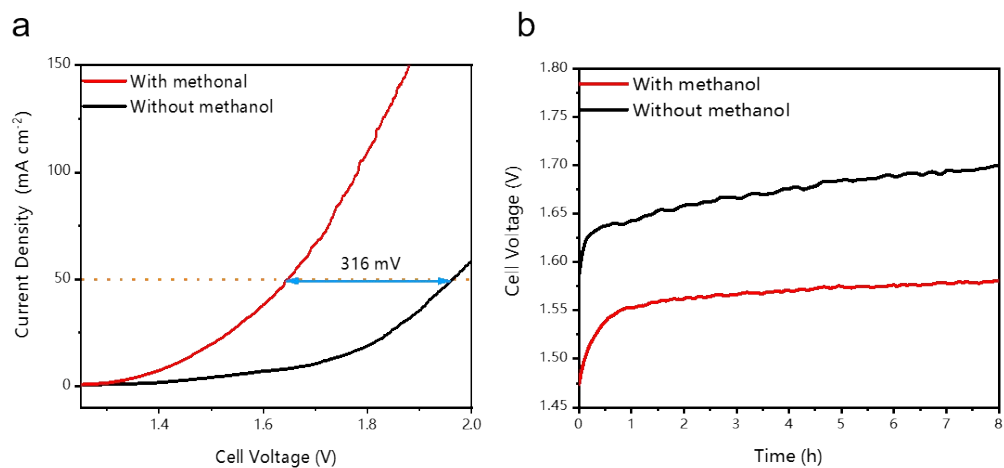


Fig. S15 (a) Comparison of LSV curves of S-NiCo-LDH as cathode and anode with and without 1 M methanol in electrolyte in single cell. **(b)** Stability test of the S-NiCo-LDH as cathode and anode at a current density of 20 mA cm⁻² in 1 M KOH containing.

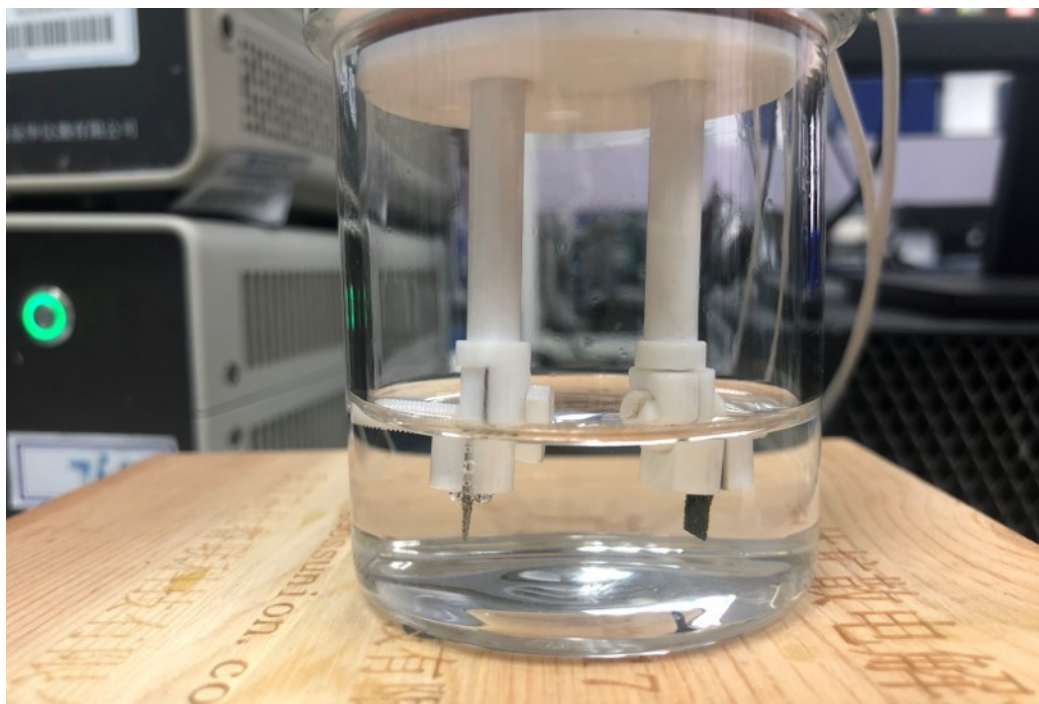


Fig. S16 Digital photo of the electrolysis cell under two-electrode system. Left electrode is cathode electrode and the right electrode is the anode electrode.

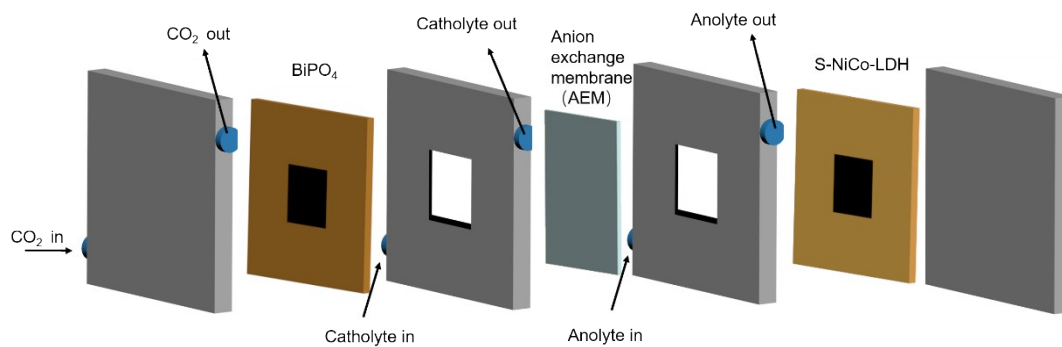


Fig. S17 Schematic illustration of the flow cell configuration to produce formate on the triple-phase boundary of the gas diffusion electrode.

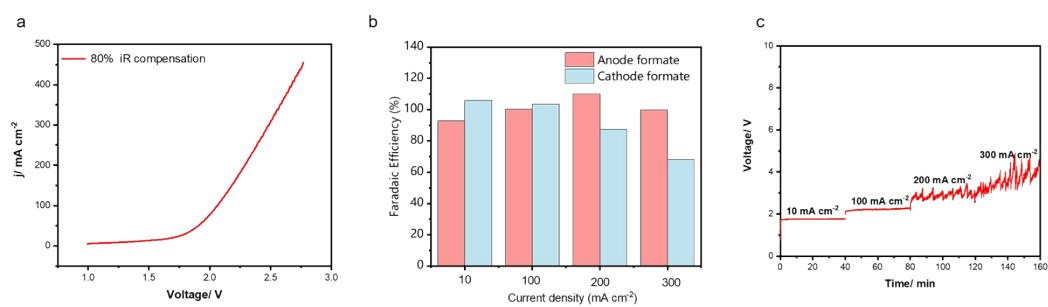


Fig. S18 (a) LSV curves of the constructed MOR || CO₂RR full cell based on the S-NiCo-LDH as anode and BiPO₄ derived nanosheets as cathode. **(b)** The calculated FEs of formate for different current density at cathode and anode, respectively. **(c)** Chronopotentiometry (CP) curves at different current densities.